Journal Pre-proof

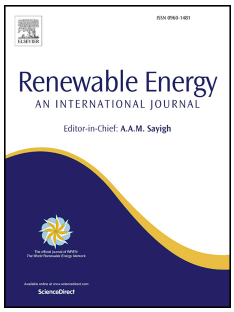

Graphene oxide – Based supercapacitors from agricultural wastes: A step to mass production of highly efficient electrodes for electrical transportation systems

R. Tamilselvi, M. Ramesh, G.S. Lekshmi, Olha Bazaka, Igor Levchenko, Kateryna Bazaka, M. Mandhakini

PII: S0960-1481(19)31765-3

DOI: https://doi.org/10.1016/j.renene.2019.11.072

Reference: RENE 12620

To appear in: *Renewable Energy*

Received Date: 9 May 2019

Revised Date: 20 September 2019

Accepted Date: 14 November 2019

Please cite this article as: Tamilselvi R, Ramesh M, Lekshmi GS, Bazaka O, Levchenko I, Bazaka K, Mandhakini M, Graphene oxide – Based supercapacitors from agricultural wastes: A step to mass production of highly efficient electrodes for electrical transportation systems, *Renewable Energy* (2019), doi: https://doi.org/10.1016/j.renene.2019.11.072.

Graphene oxide – based supercapacitors from agricultural wastes: a step to mass production of highly efficient electrodes for electrical transportation systems

R. Tamilselvi[1], M. Ramesh[2], G. S. Lekshmi[1], Olha Bazaka[3], Igor Levchenko[4], Kateryna Bazaka[3,4] and M Mandhakini[1*]

[1] *Center for Nanoscience and Technology, Anna University, Chennai, 600 025, India*
[2] *Functional Materials Division, CSIR-Central Electrochemical Research Institute, Karaikudi, 630003, India*
[3] *School of Chemistry, Physics and Mechanical Engineering, Queensland University of Technology, Brisbane, Queensland, 4000, Australia*
[4] *Plasma Sources and Application Centre/Space Propulsion Centre Singapore, NIE, Nanyang Technological University, 637616, Singapore*
[*] *mandhakini7@gmail.com*

Graphical Abstract

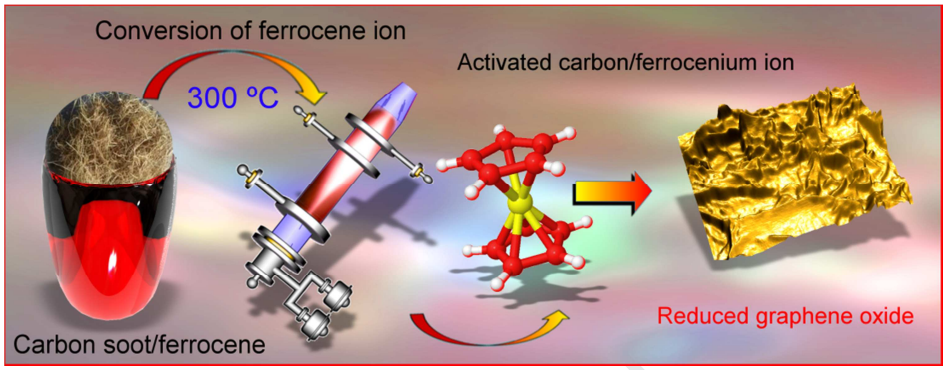

Resubmitted to Renewable Energy. Revised version RENE-S-19-02700R1

Graphene oxide – based supercapacitors from agricultural wastes: a step to mass production of highly efficient electrodes for electrical transportation systems

R. Tamilselvi[1], M. Ramesh[2], G. S. Lekshmi[1], Olha Bazaka[3], Igor Levchenko[4,3], Kateryna Bazaka[5,3,4] and M. Mandhakini[1*]

[1] *Center for Nanoscience and Technology, Anna University, Chennai, 600 025, India*

[2] *Functional Materials Division, CSIR-Central Electrochemical Research Institute, Karaikudi, 630003, India*

[3] *School of Chemistry, Physics and Mechanical Engineering, Queensland University of Technology, Brisbane, Queensland, 4000, Australia*

[4] *Plasma Sources and Application Centre/Space Propulsion Centre Singapore, NIE, Nanyang Technological University, 637616, Singapore*

[5] *Research School of Electrical, Energy and Materials Engineering, The Australian National University, ACT 2601, Australia*

[*] *Corresponding author. E-mail address: mandhakini7@gmail.com*

ABSTRACT

Supercapacitors and other innovative devices for electric energy generation and storage could significantly improve ecological situation in large densely populated cities. However, for this to become reality, supercapacitors should be produced *en masse* via a clean, green technology from the ecologically friendly material, preferably from abundant, sustainable resources, such as agricultural waste that is a by-product of other technological cycles. Many types of agricultural waste could be considered as an abundant, low-cost carbon source for large-scale fabrication of graphene-type materials. Here, we demonstrate that widely available coconut waste can be efficiently converted into reduced graphene oxide via simple catalytic oxidation using ferrocene as an efficient and low-cost catalyst. The structure and morphology of the as-prepared materials were characterized by XRD, SEM, and TEM techniques. The results confirmed the formation of high-quality reduced graphene oxide. The as-prepared graphene oxide was then analyzed as an electrode material for supercapacitor applications. We have found that the material exhibits high performance as an electric double layer capacitor (EDLC) and demonstrates excellent cyclic stability. Therefore, the reduced graphene oxide prepared via a simple, green process from this type of agricultural waste could be a good candidate of the supercapacitor electrodes.

Keywords: Reduced graphene oxide, agricultural waste, electrochemical performance, cyclic stability.

1. Introduction

Raw biomass and agricultural waste present an abundant, carbon-neutral and affordable source of carbon for the synthesis of value-added carbonaceous materials [1-3]. Recently, reforming of biomass into valuable nanoscale products for high performance electronic devices, water purification and energy applications have gained a lot of interest from scientists and industry globally in an effort to identify affordable new precursors for the commercial manufacture of graphene-type materials [4-7]. To date, successful synthesis of graphene from agricultural wastes and raw materials such as rice husk, hemp, glucose, foodstuff, paper cups, and even insects have been demonstrated [8-11].

Among graphene-type materials, reduced graphene oxide (rGO) has attracted attention of the scientific community as a promising candidate for electronics and energy devices [12,13]. Reduced graphene is a single-atom thick sheet of sp2 hybridized carbon atoms arranged in a honeycomb lattice structure with outstanding properties such as high surface area, high electrical conductivity, good chemical stability, and excellent mechanical strength [14-18]. Because of these unique properties, material platforms based on reduced graphene and rGO have been applied in ultra-filtration, wastewater treatment, photocatalysis, and as a material for energy storage and conversion devices, including supercapacitors, solar cells, fuel cells, and batteries.

As an energy storage device, supercapacitors are an effective and practical technology for electrochemical energy conversion and storage for hybrid electric vehicles, electric vehicles, portable electronic devices and backup power systems. Supercapacitors can be classified as electrostatic double-layer capacitors (EDLC) or pseudocapacitors on the basis of their storage mechanism. EDLC capacitors store the energy by charge accumulation at the electrode/electrolyte interface, whereas pseudocapacitors store the energy by the redox reaction over the surface of the electrode material. Carbon based materials, such as graphene (G), reduced graphene oxide (rGO), and graphene oxide (GO) present an attractive alternative to transition metal oxide, metal sulfides and conducting polymers for supercapacitor applications [19] due to an attractive combination of large surface area, 2D sheet morphology [20] and electrical conductivity combined with unusual mechanical properties and good dispersion performance [21,22] rGO is the best example of an EDLC supercapacitor which stores the energy by means of charge accumulation [21-25], with material performance strongly linked to the quality of rGO material used.

Currently used methods for the synthesis of high-quality G, GO and rGO are typically complex, require the use of specific processing environments and often involve the use of highly purified and potentially hazardous chemicals [26-30]. This presents a significant environmental and economical challenge31 and drives the search for simpler, more sustainable synthesis techniques that can utilize diverse minimally processed carbon sources without compromising the quality of the end product [28,32]. Wet chemistry-based techniques successfully used for the production of useful materials from waste products include sol-gel processes, layer-by-layer assembly, electrospinning, thermal decomposition, solvothermal and microwave-assisted synthesis [33,34]. However, the common drawback of these wet techniques is the generation of by-products that contaminate the useful product, in our example, the graphite layers [35,36].

In this work, we describe a novel method for the synthesis of rGO from the biomass with the use of ferrocene as a catalyst. Although simple, this approach can be used to successfully produce a valuable nanostructured material with good quality, and importantly, as very low temperature of 300 °C. This is in contrast to wet techniques, where it might be difficult to eliminate the defects on the carbon basal plane due to the harsh nature of the reducing agents and agglomeration of nanomaterials in organic solvents. Processing temperature, band gap and amount of oxygen in the carbon precursor also play an important role in defining the properties of rGO. On one hand, higher temperatures reduce oxygen concentration in rGO, but on the other hand they introduce defects in the lattice structure of rGO [37]. For this reasons, significant efforts have been devoted to reducing the processing temperature used for GO reduction to favor defect-free rGO sheet production.

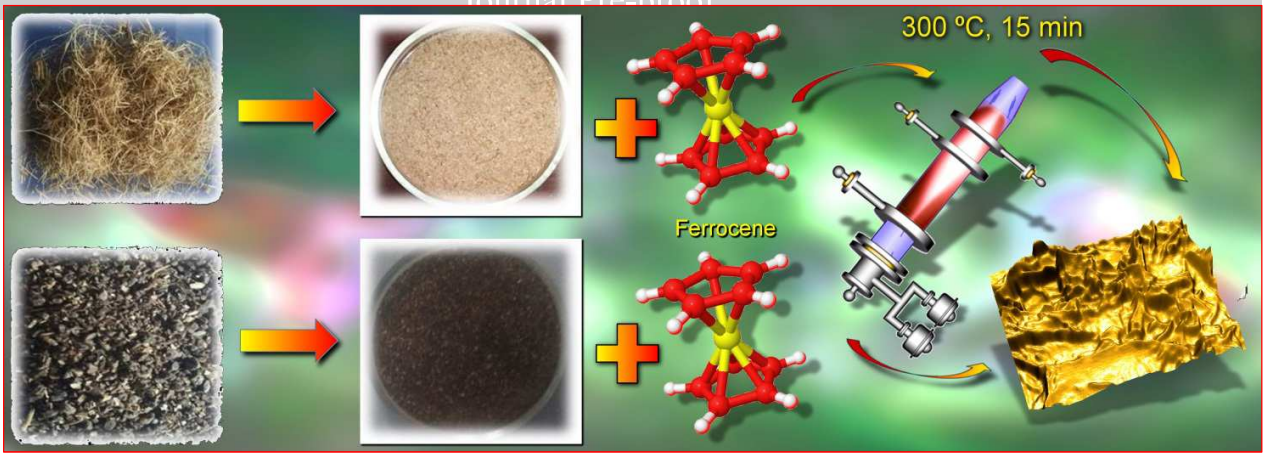

Fig. 1. Synthesis of reduced graphene oxide via simple catalytic oxidation in a muffle furnace using ferrocene as an efficient and low-cost catalyst and coconut coir or coconut shell as a carbon source. Temperature and time are dominant parameters in determining the properties of the resulting material. This simple, environmentally friendly process that uses a natural, abundant raw product may be scaled up for mass production of graphene oxide electrodes for electrical transportation systems.

Mas'udah *et al.* reported the production of reduced graphene oxide by heating old coconut for 3h at 400 °C. In their study, they proposed that the constituents of coconut shell, namely cellulose ((C6H10O5)n) and hemicellulose, have bonds related to the hexagonal crystal structure of graphene, and hence these constituents can potentially be reduced in order to get a single layer of graphene-type material [38]. Synthesis of GO via direct oxidation of sugarcane bagasse under muffled atmosphere with ferrocene as a catalyst was reported by Somanathan *et al.* [14], however the performance of thus-fabricated material and the effect of processing conditions on the fundamental characteristics of rGO were not studied.

In this work, we show that rGO synthesized directly from an agricultural waste (coconut shell and coconut coir) via direct carbonization in muffled furnace in the presence of ferrocene as an oxidizing catalyst is a strong candidate to be used as an electrode material in supercapacitor devices. By completing a survey on the effect of processing parameters on the properties of rGO, we also show that processing temperature and time are the dominant parameters in determining the properties of the resulting material. We show that optimization of these parameters allows us to synthesize high quality rGO within 15 min.

This technology, which is based on cheap materials and processes and utilizes waste as the input carbon source, could be extremely important for the commercial scale fabrication of affordable yet sophisticated nanomaterials including reduced graphene oxides to underpin the development of future nanoscale electronics and wearable systems for applications on Earth and even in space [39–45].

2. Materials and Methods

2.1. Materials

This study utilized two types of agricultural waste, namely coconut coir and coconut shell. Potassium hydroxide (KOH, analytical reagent grade) was obtained from Fisher. Carbon black (CB, 99.9900%), ferrocene and N-methyl-2-pyrrolidinone (NMP, 99%) were obtained from SRL Chemicals Ltd. (Mumbai, India). Poly(vinylidene fluoride) (PVDF) was purchased from Scientific Polymer Products, Inc. (Ontario, the United States).

2.2. Methods

2.2.1. Preparation of Reduced Graphene Oxide

The typical procedure for the synthesis of rGO (**Figure 1**) involves simple catalytic oxidation of agricultural waste [14]. Coconut shell and coconut coir were first crushed and ground in order to produce a powder. Subsequently, the carbonization was conducted by using 0.5 g of thus-prepared powder by mixing it with 0.1 g of ferrocene and placing it in a muffle furnace for 15 min at 300 °C under atmospheric (air) conditions, and then allowing it to cool to room temperature. Previous studies employing a similar catalytic mechanism of conversion of the complex carbon precursor to GO suggested the initial conditions for our study, specifically the proportion of the carbon source to the catalyst [14]. Subsequent optimization process confirmed the suitability of these parameters to enable efficient rate of conversion as well as high quality of thus-produced graphene oxide material. Of particular interest was reducing the carbonization temperature to further improve the environmental credentials of this approach without sacrificing the quality of the material. However, reducing the temperature to 200−250 °C resulted in the partial oxidation of the waste material to graphene oxide, and formation of mainly graphite-like material, as confirmed by XRD. Since in this experiment, the reforming was performed in air (in the presence of oxygen), increasing the temperature beyond 300 °C would have potentially led to a substantial mass loss and decomposition of GO material. For this reason, carbonization temperature of 300 °C was chosen for all subsequent experiments as it allowed for full oxidation of coconut waste into graphene oxide, producing a well graphitized 2D material structure made of GO sheets. This resulted in the formation of a black colored product. For easy identification, the materials were labeled as CCF and CSF to represent rGO from coconut coir and rGO from coconut shell, respectively.

2.2.2. Preparation of Reduced Graphene Oxide Electrodes

The composite electrodes were prepared by combining precisely weighed amounts of the active materials (80% or 8 mg), carbon black (10% or 1 mg), and polyvinylidene difluoride (PVDF) (10% or 1 mg) slurred with N-methyl-2-pyrrolidone (NMP). The slurry was coated over a nickel plate and dried for 12 h at 100 °C in an oven.

2.3. Proposed mechanism for the formation of rGO from agriculture waste

The chemical composition of coconut coir includes cellulose, lignin, pectin, and hemicellulose in various proportions that are determined by the species, origin, age and time of harvest, among other considerations [46]. Coconut shell waste also consists of lignin, cellulose, hemicellulose, water and ash [47]. Due to multicomponent, complex nature of the carbon source, it is likely that the mechanism of reforming is complex, and includes a large number of chemical reactions that may take place simultaneously or consecutively. Heating of the carbon precursor would lead to evaporation of water and highly volatile substances, such as methanol, formic and acetic acid, and partial decomposition and volatilization of carbon compounds, which would also increase the porosity of the solid material. Previous studies of thermal decomposition of commonly found hemicelluloses, *i.e.* arabinogalactan, arabinoxylan, β-glucan, galactomannan, glucomannan, xyloglucan, xylan, as well as cellulose have shown a substantial mass loss between 200 and 250 °C, with mass loss rate maxima between 292 °C and 326 °C [48]. Depending on the temperature and the chemistry of the initial carbon source, the volatiles may comprise any combination of condensable and non-condensable molecules, including CO, CO2, smaller molecules species including alcohols, aldehydes and acids, as well as heavier structures, *e.g.* furan-ring products and anhydrosugars [48].

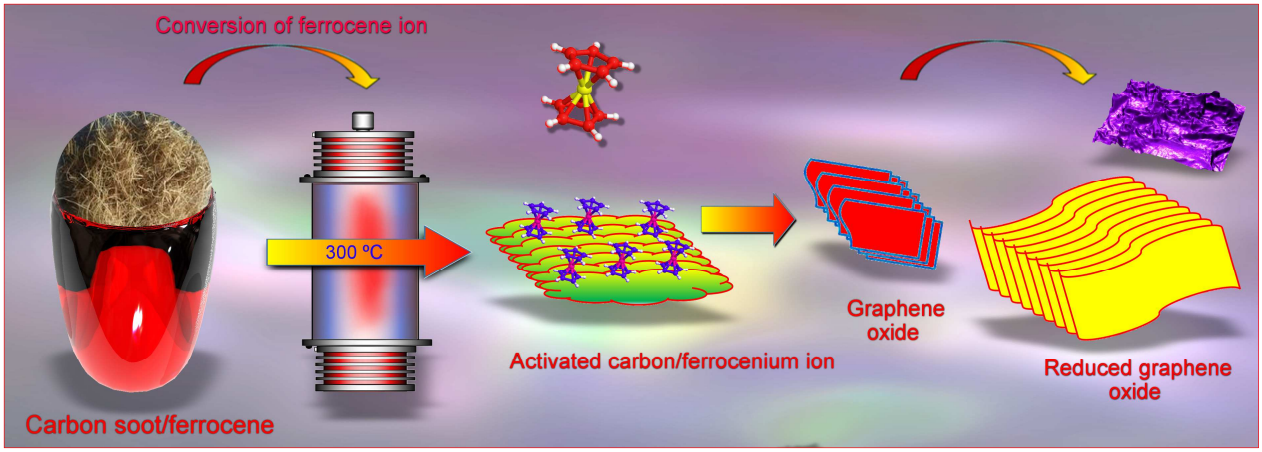

Fig. 2. Mechanism of reduced graphene oxide growth. Carboxylic groups are removed thermally to reduce graphene during a short annealing step. During extended annealing, the removal of carboxylic and epoxy groups was accompanied by carbon loss and associated defect formation, thus resulting in the formation of CO_2 and CO by-products.

At the same time, above 249 °C, ferrocene exceeds its boiling point [49], which allows it to effectively reach and interact with the increasingly porous carbon material and catalyze the secondary reactions with volatilized and solid carbons. At this point, ferrocene can induce a wide range of transformations into the residual carbon molecules by injection of an electron. Ferrocene itself can undergo a reversible one-electron oxidation reaction to produce ferrocenium ions, which can take part in both hole catalysis and electron catalysis [50]. In some instances, ferrocenium ions have been proposed to act as a mild lewis acid catalyst to promote oxidation of carbon soot [50]. A combination of these reaction lead to the formation of graphene-like structures of sp^2 hybridization, as expected for rGO. This is confirmed by FTIR and XRD results, which are in agreement with the results previously reported by Somanathan *et al.* who showed that GO was formed by heating the sugarcane bagasse for 10 min at 300 °C [14], and those reported by Sa *et al.* who have used ferrocene for the production of rGO from GO in the presence of HNO_3 acid [51]. In the latter example, the acid facilitated the di-nitration of ferrocene to ferrocenyl dinitric acid, and excess HNO_3 driven generation of Fe^{3+}, which works as a principal catalytic agent due to its ability to act as a strong coordinator to the oxiranes (epoxides) $C_6H_{12}O_3$, which in turn reduce to alkenes. A number of acids, including formic, ferulic and acetic acid are naturally produced during thermal decomposition of cellulosic biomass [48], potentially contributing to in situ reduction of GO via opening of epoxides into diols in presence of acids, further being reduced to alkenes in presence of excess acid [51].

Thus-formed graphene oxide is then thermally reduced via elimination of carboxylic groups (**Figure 2**). This step is achieved when GO obtained as a result of oxidation process of soot is subjected to thermal annealing for additional 5 min, which is sufficient to reduce GO. The successful reduction is confirmed by the XRD, FTIR and Raman analysis. When the annealing step was extended to 15 min (at 300 °C), the removal of carboxylic and epoxy groups was accompanied by carbon loss and associated defect formation, leading to the formation of by-products such as CO_2 and CO [21,32]. Both CO_2 and CO are considered as environmental pollutants, and therefore every effort is made to minimize their generation during material synthesis and processing.

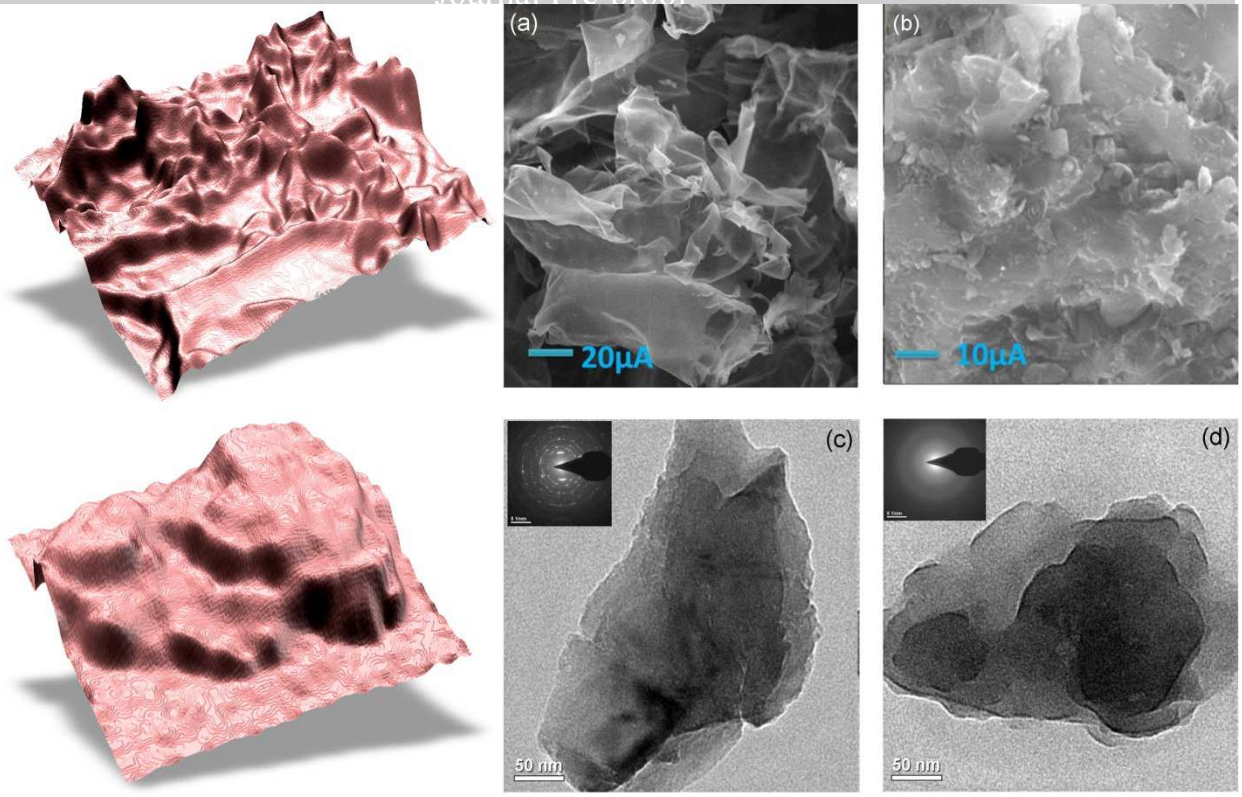

Fig. 3. SEM images of reduced graphene oxide from CC (a) and CS (b). TEM images of reduced graphene oxide from (c) CC and (d) CS. The grown materials feature virtually a sheet-like morphology, which indicates the formation of reduced graphene oxide.

2.4. Material characterization

The structural characterization of the carbonized materials was performed by X-ray diffraction (XRD) analysis using a Rigaku Minflux II-c X-ray diffractometer with Cu K radiation of wavelength 0.154 nm, Raman spectroscopy (AGILTRON1 (QEB1920)). The morphology of the sample was investigated using the scanning electron microscopy (SEM) and transmission electron microscopy (TEM). Fourier transform infrared (FT-IR) spectra were collected on a Shimadzu IRPrestige-21 infrared spectrometer over the range of 4000-500 cm^{-1}. The UV-vis adsorption spectra were recorded using a UV-vis-NIR spectrophotometer (Cary 5E) in the wavelength ranging from 200-1100 nm. The surface composition was investigated using X-ray photoelectron spectroscopy (XPS) instrument filled with HSA 15000 power supply. The cyclic voltammetry, galvanostatic charge/discharge and electrochemical impedance spectroscopy studies were performed using an electrochemical analyzer (Biologic VMP3).

2.5. Preparation of electrodes and electrochemical characterization

All the electrochemical measurements were performed in a standard Biologic VSP multichannel potentiostat. Cyclic voltammetry (CV) data were analyzed with various scan rates ranging from 10-500 mV/s, and galvanostatic charge-discharge studies were performed at different current density ranging from 0.025-1 mA. Electrochemical impedance spectroscopy (EIS) studies were performed using an electrochemical work station Bio-Logic (VSP). The capacitive behavior of the materials was examined using a three-electrode system in a 2M potassium hydroxide (KOH) aqueous electrolyte. A platinum rod, a saturated calomel electrode and rGO electrode were used as the counter electrode, reference electrode and working electrode, respectively. The specific capacitance (C_s) was derived from a galvanostatic curve, which can be calculated from equation (1) as follows:

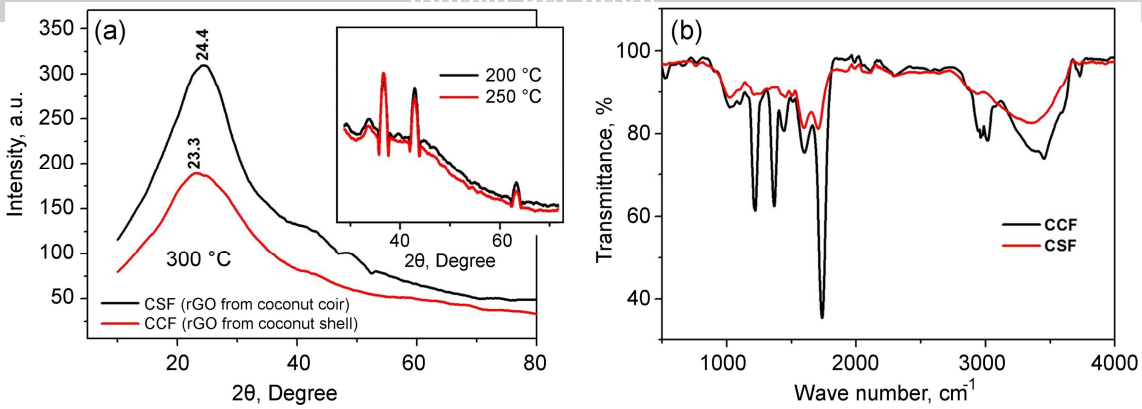

Fig. 4. (a) XRD patterns of rGO derived from CC (coconut coir) and CS (coconut shell). Inset shows strong peaks at about 40°, evidencing graphite structure produced at 200 and 250 °C, while the material produced at 300 °C does not feature these peaks but instead, evidences the graphene structures. The diffraction peaks are broad and intense, indicating the formation of nano-sized materials. The peak at 2θ = ~ 24° is the (002) crystal plane of reduced GO, and all the samples demonstrate the diffraction peak at 2θ = 42°, corresponding to the (100) lattice plane. (b) FTIR spectra of CCF and CSF. The FTIR spectra confirm the formation of oxygen containing groups.

$$C_s = \int I\, dt/\, mv. \tag{1}$$

The specific capacitance (C_s) derived from the galvanostatic curve can be calculated from equation (2) as follows:

$$C_s = It/\, mV, \tag{2}$$

where I is the discharge current (A), t is the discharge time (s), m is the weight of the active material (g) and V is the potential range, v is the scan rate (mV/s).

3. Results and Discussion

3.1. SEM, TEM, AFM, FTIR, Raman and XRD Characterization

The typical surface morphology of the resulting materials is shown in **Figure 3**. Both types of materials are shown to have virtually a sheet-like morphology, which indicates the formation of rGO. TEM characterization was used to confirm the structure of thus-synthesized materials. TEM images show that rGO produced by this method are thin sheets with a few layers.

Figure 4a represents the typical XRD patterns of the as-prepared samples. The observed X-ray diffractions peaks are found to be broad and intense, which is indicative of the formation of nano-sized materials. The XRD diffraction peak at 2θ = ~ 24° is indexed to the (002) crystal plane of rGO, and all the samples exhibit the diffraction peak at 2θ = 42°, corresponding to the (100) lattice plane of rGO [52]. The diffraction peak appears at 23.3°, 24.4° relevant to the (002) plane for CCF and CSF, respectively. The (002) peak clearly shifts to a larger angle corresponding to a smaller interlayer distance [53]. In general, the d spacing of graphite is 0.3354 nm, whereas the d spacing of turbostratic carbon is about 3.38– 3.41 Å [41]. The interlayer distance in CCF samples is ~ 3.8 Å and for CSF samples it is 3.6 Å. This is because of the presence of the small amount of residual oxygen-containing functional groups or other structural defects [54,55].

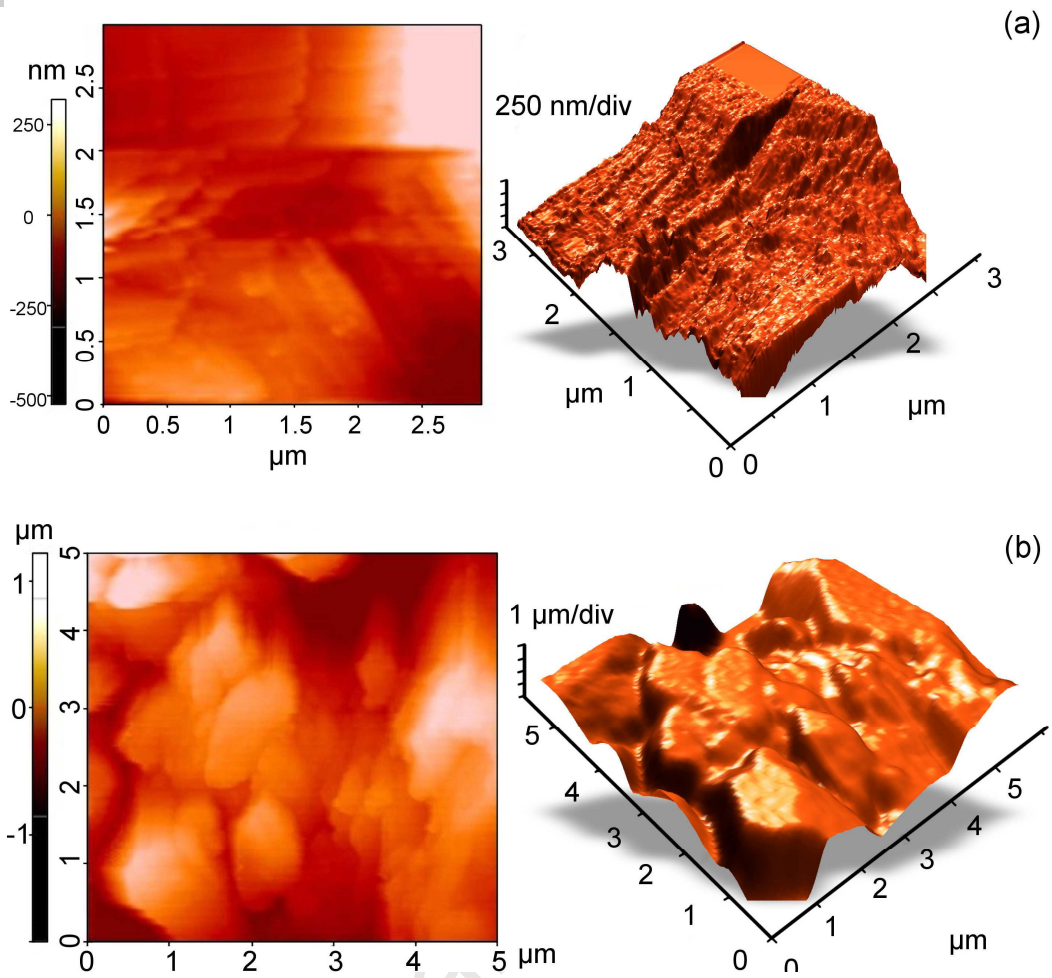

Fig. 5. Representative AFM images of surfaces of (a) CCF and (b) CSF. Due to the overlapping of sheets and ripples, the roughness of the samples are 0.166 μm and 0.335 μm for CCF and CSF, respectively. The large surface roughness of the samples is attributed to the presence of covalent C–O bonds at both top and bottom surfaces. It can also be caused by distorted sp^3 carbon lattices and adsorbed contaminants.

FTIR spectra of thus-synthesized materials shown in **Figure 4b** confirm the introduction of oxygen containing groups, such as functional hydroxyl, epoxy and carboxylic groups upon oxidation of waste biomass. A strong band at 1733 cm^{-1} is attributed to the stretching vibration modes of C=O in carboxylic acid and carbonyl groups. The peak at 1588 cm^{-1} is assigned to the skeletal vibrations of un-oxidized graphitic domains. The band at 1060 cm^{-1} is assigned to C–O (epoxy) groups while the band at 1210 cm^{-1} is usually attributed to C–OH stretching vibrations. The strong peak around 3500–4000 cm^{-1} can be attributed to the O–H stretching vibrations of the C–OH groups.

The morphological properties of the synthesized materials were studied by the atomic force microscopy. The formation of rGO sheets are shown in **Figure 5**. Due to the overlapping of sheets and ripples the roughness of the samples was estimated to be 0.166 μm and 0.335 μm for CCF and CSF, respectively. The large surface roughness in the latter sample type can mainly be attributed to the presence of the covalent C–O bonds at both the top and bottom surfaces. It can also be caused by distorted sp^3 carbon lattices and adsorbed contaminants [42].

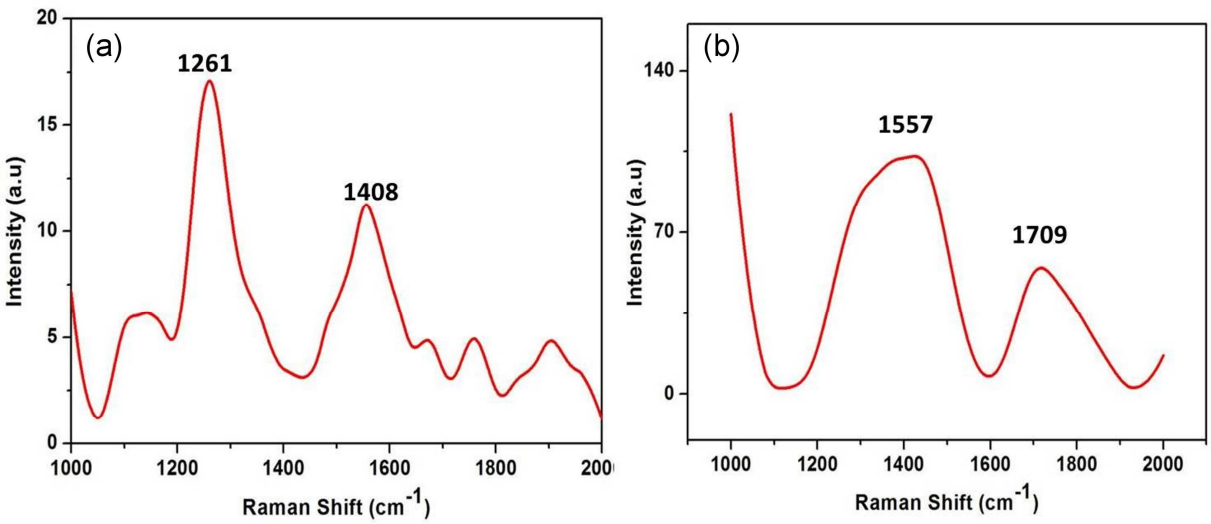

Fig. 6. Raman spectra for (a) CCF and (b) CSF. Raman technique shows that the use of two different raw materials resulted in graphene oxide with similar Raman spectra, with D band arising from the defect sites of carbon, and G band representing the sp^2 carbon. The two intense features are assigned to the D band at 1261 cm^{-1} and 1408 cm^{-1}, and the G band at 1557 cm^{-1} and 1709 cm^{-1}.

Raman spectroscopy is an efficient tool to probe the structural characteristics and properties of graphene-based materials to identify defect structures, defect densities and doping levels. The Raman spectra of rGO produced from different types of coconut waste are shown in **Figure 6**. We found that the use of two different starting material resulted in rGO with similar Raman spectra in terms of their overall shape and the positions of Raman peaks, with D band arising from the defect sites of carbon, and G band representing the sp^2 carbon. In the Raman spectra of rGO from CC and CS, two intense features are assigned to the D band at 1261 cm^{-1} and 1408 cm^{-1}, and the G band at 1557 cm^{-1} and 1709 cm^{-1}, respectively [56].

X-ray photoelectron spectroscopy was used to confirm the atomic valence states of thus-produced rGO materials. **Figure 7** show the XPS spectra for rGO obtained from CC and CS. The survey spectra mainly reveals the presence of C and O elements. XPS spectrum for C1s and O1s binding energy of rGO from CC shows an intense peak at 284.2eV attributed to carbon with sp^2 hybridization [57,58]. The C 1s spectrum displays peaks at 284.2 eV and 290.2eV corresponding to C-C, stretching (graphitic carbon) in aromatic rings and carboxylic COOH. The 290.8 eV peak corresponds to the carboxyl (-COOH). The intensity of -COOH in the C 1s spectrum is higher in CCF than CSF which indicates the higher level of reduction in CSF compared to CCF. This is in good agreement with the results obtained using FTIR. The O 1s excitation was resolved at 540.8 eV for CCF, which corresponds to the carboxylic group. For CSF, the 534 eV peak corresponds to the oxygen single bonded to the carbon atom [59].

3.2. UV-Vis absorption spectra, zeta potential and electrochemical characterization

Figure 8a shows the UV-visible spectra of CCF and CSF dispersed in deionized water. rGO obtained from CCF and CSF show the absorption peak at 260 nm, which confirms the formation of reduced graphene oxide. The absence of an absorption peak at 307 nm shows the removal of oxygen containing functional groups.

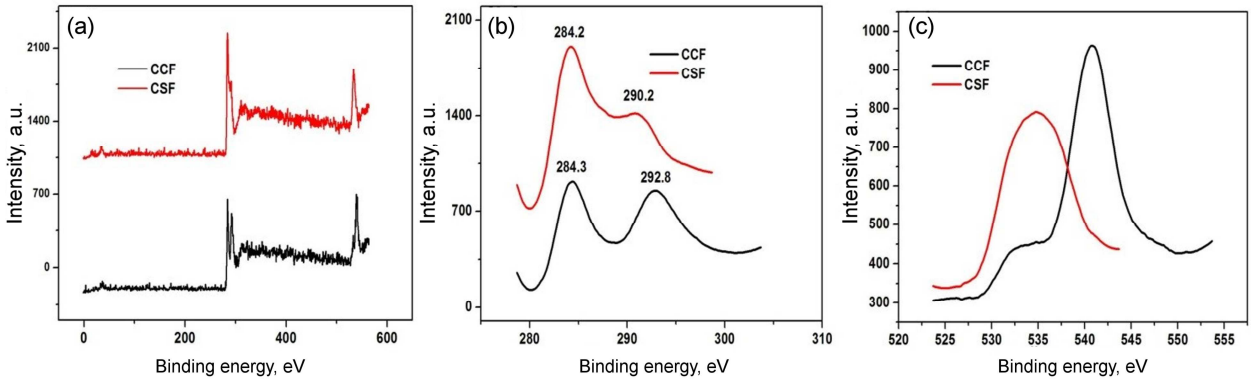

Fig. 7. XPS spectra for CCF and CSF: (a) survey spectra, (b) C1s, (c) O1s. The survey spectra reveals the presence of C and O elements, while XPS spectrum for C1s and O1s binding energy of the reduced graphene oxide from CCF shows an intense peak at 284.2 eV, attributed to carbon with sp^2 hybridization. The C 1s spectrum displays peaks at 284.2 eV and 290.2 eV corresponding to C-C, stretching in aromatic rings, and carboxylic COOH groups. The 290.8 eV peak corresponds to the carboxyl (-COOH) group.

Zeta potential measurements of rGO were carried out using a DLS instrument to calculate their stability in an aqueous medium. Zeta potential value of neutral nanoparticles is between 10 mV and +10 mV [60]. From **Figure 8b** the value of zeta potential for rGO obtained from CC and CF in the absence of ferrocene is −9.95 mV and −20 mV respectively, whereas the rGO obtained in the presence of ferrocene shows zeta potential of −28.4 mV and −33.9 mV, respectively. The materials produced in the presence of ferrocene are more stable in aqueous media, with a more anionic nature than those produced without ferrocene. These negative charges help in the charge storage mechanism of CCF and CSF [41].

To investigate the electrochemical properties of as-synthesized materials, electrochemical measurements were performed in a three electrodes system by cyclic voltammetry in order to determine the voltage windows for each electrolyte, and by chronopotentiometry at different current densities to determine the capacity and stability of the rGO-based electrodes.

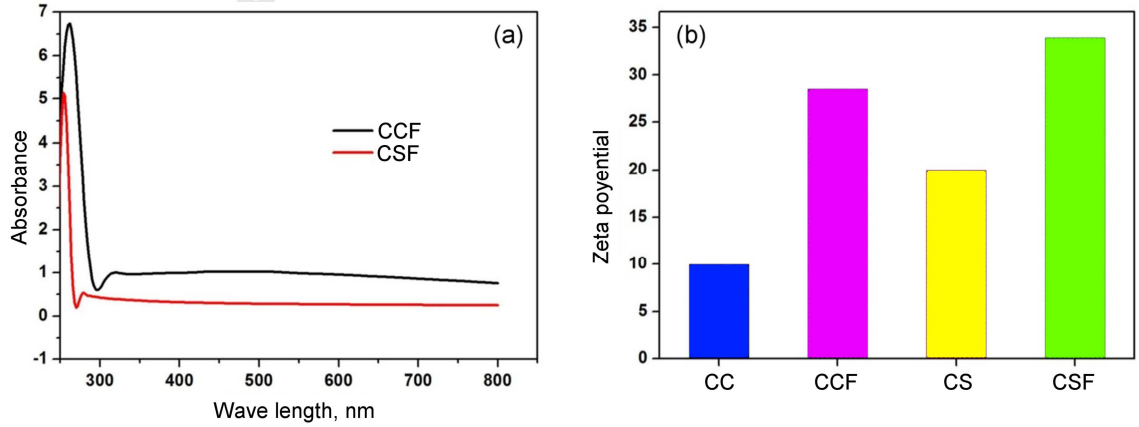

Fig. 8. (a) UV-visible spectra of CCF and CSF. (b) Zeta potential of CC and CS (without ferrocene treatment) and CCF and CSF (with ferrocene treatment). UV-visible spectra of CCF and CSF show the peak at 260 nm, which confirms the formation of reduced graphene oxide. The absence of an absorption peak at 307 nm proves the removal of oxygen containing functional groups. Zeta potential measurements show that the ferrocene treated materials are more stable in aqueous media, with a more anionic nature than those without ferrocene treatment.

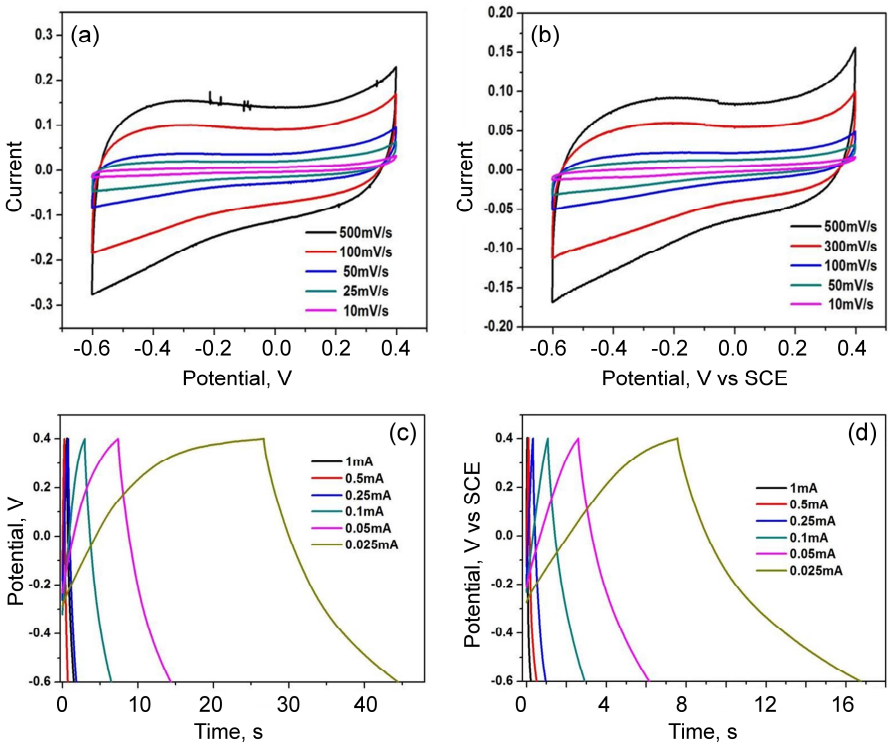

Fig. 9. Cyclic voltammograms for CCF and CSF. Charge-discharge characteristics in 2M KOH for (a) CCF and (b) CSF. The shape of the graphs confirms the EDLC behavior. As-prepared graphene oxide obtained from CS and CC can reach the maximum specific capacitance of 76.6 F/g and 114 F/g, respectively. The rGO derived from CC shows higher specific capacitance due to the highly crystalline nature of rGO. The rGO derived from CS shows lower specific capacitance.

Figures 9a, b show cyclic voltammograms obtained using CCF and CSF electrodes at 500, 300, 100, 50, 25, 10 mV s^{-1}. The rectangular shape of the graphs confirms the EDLC behavior of the materials. The specific capacitance (C_s) is estimated from *C-V* curve using equation (1). As-prepared rGO obtained from CS and CC can reach the maximum specific capacitance of 76.6 F/g and 114 F/g, respectively, at a scan rate of 10 mV/s. The increasing sweep current with the scan rate confirms the good EDLC capacitive nature of the rGO electrodes. When comparing the performance of rGO derived from CC and CS, CCF shows higher specific capacitance due to the highly crystalline nature of rGO as inferred from TEM and SAED results. However, CSF shows lower specific capacitance due to the turbostratic nature of rGO derived from CS. The turbostratic carbon is an intermediate of amorphous carbon and a crystalline graphene structure, and is believed to possess fewer vacancies thus resulting in lower ion desolvation and lower energy storage capacity [53-62].

The electrochemical properties and charge storage capacity of the carbonized materials were further investigated using galvanostatic charge-discharge measurements. **Figures 9c and 9d** show the galvanostatic charge-discharge characteristics of the carbonized materials in 2M KOH electrolyte. GCD curves showed a triangular shape, the specific capacitance obtained by chronopotentiometry decreased rapidly as current density increased. The specific capacitances values at different current densities were also measured from the GCD curve. It clearly shows that the CCF electrode has a maximum specific capacitance of 111.1 F/g compared to that of CSF at 60.2 F/g. Specific capacitance was observed to decrease with increasing current density which could be due to insufficient time for the electrolyte ions to diffuse into the inner pores of carbonized materials. In addition, it is further observed that the specific capacitance depends on the electrolytes used for the measurements.

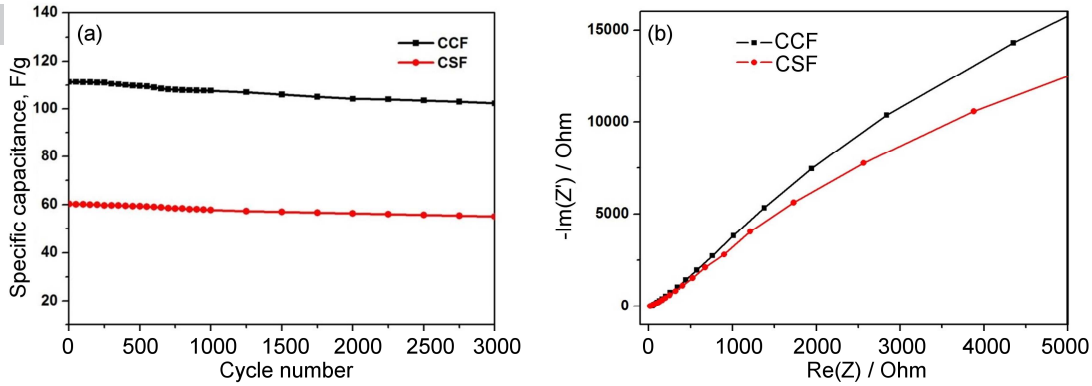

Fig. 10. (a) Cyclic stability of the electrodes at 0.024 mA cm^{-1}. The specific capacitance decreases gradually with the cycle number, and 3% of loss was detected for the corresponding reduced graphene oxide obtained from CC and CS, thus substantiating the excellent electrochemical stability of the electrode materials. (b) EIS measurements for CCF and CSF. At low frequency, the vertical slope corresponds to the Warburg impedance.

Cyclic stability of the electrode is tested by continuous charging/discharging over 3000 cycles at the constant current density of 0.024 mA cm^{-1} showed in **Figure 10a**. The specific capacitance value decreases gradually with increasing the cycle number; only about 3% of capacity loss is observed for the corresponding reduced graphene oxide obtained from CC and CS. This substantiates the excellent electrochemical stability of the electrode materials.

The electrochemical performance of the reduced graphene oxide is further confirmed with electrochemical impedance analysis. Electrochemical impedance tests were carried out to evaluate the charge transfer and electrolyte diffusion in the electrode/electrolyte interface, as shown in **Figure 10b**. As shown in the figure, the negligible semicircle like region at high frequencies represents low equivalent series resistance (ESR). Further, in the low frequency region, the vertical slope corresponds to the Warburg impedance. The electrode exhibits a more vertical line at low frequency, illustrating better capacitive behavior and lower diffusion resistance of the prepared reduced graphene oxide.

Conclusions

In this work, the reduced graphene oxide was successfully synthesized by a simple oxidizing method from coconut shell and coconut coir at low temperature. rGO fabricated under optimized conditions (300 °C, 15 min) were tested as a supercapacitor electrode. The SEM and TEM images of the materials produced from both types of biomass revealed the formation of multi-layer rGO sheets. XRD, XPS and Raman spectra confirmed that thus-produced materials were rGO. From the electrochemical studies, the highest specific capacitance of 111.1 F/g and 60.2 F/g in 2M KOH electrolyte was observed for CCF and CSF, respectively. In addition, they show a very stable performance of 99% over 3,000 charge and recharge cycles. Our studies indicate that this method presents an efficient pathway for rapid synthesis of high quality rGO with properties that make it suitable for applications in high performance flexible supercapacitor devices.

Acknowledgements

The authors are grateful to Mr. Jaspreet Singh and Mr. U.K. Goutam, Scientific officers, RRCAT, Indore, for providing XPS analysis.

444 **References**

[1] K. Bazaka, M. V. Jacob, K. Ostrikov, Sustainable life cycles of natural-precursor-derived nanocarbons, Chem. Rev. 116 (2016) 163–214.

[2] V. F. S. Filho, L. Batistella, J. L. F. Alves, J. C. G. Silva, C. A. Althoff, R. F. Peralta, M. Moreira, H. J. José, Evaluation of gaseous emissions from thermal conversion of a mixture of solid municipal waste and wood chips in a pilot-scale heat generator, Renew. Energy 141 (2019) 402-410.

[3] V. Vadery, S. K. Cherikkallinmel, R. M. Ramakrishnan, S. Sugunan, B. N. Narayanan, Green production of biodiesel over waste borosilicate glass derived catalyst and the process up-gradation in pilot scale, Renew. Energy 141 (2019) 1042-1053.

[4] M. Kouhi, K. Shams, Bulk features of catalytic co-pyrolysis of sugarcane bagasse and a hydrogen-rich waste: The case of waste heavy paraffin, Renew. Energy 140 (2019) 970-982.

[5] G. Selvaraju, N, K, A, Bakar, Process conditions for the manufacture of highly micro-mesoporous eco-friendly activated carbon from artocarpus integer bio-waste by steam activation, J. Taiwan Inst. Chem. Eng. 93 (2018) 414–426.

[6] M. V Jacob, R. S. Rawat, B. Ouyang, K. Bazaka, D. S Kumar, D. Taguchi, M. Iwamoto, R. Neupane, O. K. Varghese, Catalyst-free plasma enhanced growth of graphene from sustainable sources, Nano Lett. 15 (2015) 5702-5708.

[7] I. Levchenko, K Ostrikov, Plasma/ion-controlled metal catalyst saturation: Enabling simultaneous growth of carbon nanotube/nanocone arrays, Appl. Phys. Lett. 92 (2008) 063108.

[8] M. J. Ahmed, Application of agricultural based activated carbons by microwave and conventional activations for basic dye adsorption: Review, J. Environ. Chem. Eng. 4 (2016) 89–99.

[9] K. Bazaka, M. V. Jacob, R. J. Crawford, E. P. Ivanova, Plasma-assisted surface modification of organic biopolymers to prevent bacterial attachment, Acta Biomater. 7 (2011) 2015-2028.

[10] S. Wong, N. Ngadi, I. M. Inuwa, O. Hassan, Recent advances in applications of activated carbon from biowaste for wastewater treatment: A short review, J. Cleaner Product. 175 (2018) 361–375.

[11] H. Chen, Y.-C. Guo, F. Wang, G. Wang, P.-R. Qi, X.-H. Guo, B. Dai, F. Yu, An activated carbon derived from tobacco waste for use as a supercapacitor electrode material, New Carbon Mater. 32 (2017) 592-599.

[12] I. Levchenko, K. Bazaka, T. Belmonte, M. Keidar, Advanced Materials for Next Generation Spacecraft, Adv. Mater. 30 (2018) 1802201.

[13] I. Levchenko, K. Bazaka, M. Keidar, S. Xu, J. Fang, Hierarchical multi-component inorganic metamaterials: Intrinsically driven self-assembly at nanoscale, Adv. Mater. 30 (2018) 1702226.

[14] T. Somanathan, P. K. Prasad, K. Ostrikov, A. Saravanan, M. Vemula, Graphene Oxide Synthesis from Agro Waste, Nanomaterials 5 (2015) 826-834.

[15] H. Song, L. Zhang, C. He, Y. Qu, Y. F. Tian, Y. Lv, Graphene sheets decorated with SnO_2 nanoparticles: in situ synthesis and highly efficient materials for cataluminescence gas sensors, J. Mater. Chem. 21 (2011) 5972–5977.

[16] Y. C. Si, E. T. Samulski, Exfoliated graphene separated by platinum nanoparticles, Chem. Mater. 20 (2008) 6792–6797.

[17] G. Lu, S. Park, K. Yu, R. S. Ruoff, L. E. Ocola, D. Rosenmann, Toward practical gas sensing with highly reduced graphene oxide: A new signal processing method to circumvent run-to-run and device-to-device variations, J. Chen. ACS Nano 5 (2011) 1154–1164.

[18] C. Lee, X. Wei, J. W. Kysar, J. Hone, Measurement of the elastic properties and intrinsic strength of monolayer graphene, Science 321 (2008) 385–388.

[19] N. Yu, M. Q. Zhu, D. Chen, Flexible all-solid-state asymmetric supercapacitors with three-dimensional $CoSe_2$/Carbon cloth electrodes, J. Mater. Chem. A 3 (2015) 7910–7918.

[20] B. B Wang, D. Gao, I. Levchenko, K. Ostrikov, M. Keidar, M. K. Zhu, K. Zheng, B. Gao, Self-organized graphene-like boron nitride containing nanoflakes on copper by low-temperature N_2+H_2 plasma, RSC Advances 6 (2016) 87607-87615.

[21] D. W. Wang, F. Li, M. Liu, H.-M. Cheng, Improved capacitance of SBA-15 templated mesoporous carbons after modification with nitric acid oxidation, New Carbon Mater. 22 (2007) 307–314.

[22] G. Beaucage, H. K. Kammler, S. E. Pratsinis, Particle size distributions from small-angle scattering using global scattering functions, J. Appl. Crystallogr. 37 (2004) 523-535.

[23] A. Jain, S. K. Tripathi, Nano-porous activated carbon from sugarcane waste for supercapacitor application, J. Energy Storage 4 (2015) 121–127.

[24] J. R. Miller, P. Simon, Electrochemical capacitors for energy management, Science 321 (2008) 651-652.

[25] W. Li, H. Probstle, J. Fricke, Electrochemical behavior of mixed CmRF based carbon aerogels as electrode materials for supercapacitors, J. Non-Cryst. Solids 325 (2003) 1–5.

[26] D. H. Seo, A. E. Rider, A. Das Arulsamy, I. Levchenko, K. Ostrikov, Increased size selectivity of Si quantum dots on SiC at low substrate temperatures: An ion-assisted self-organization approach, J. Appl. Phys. 107 (2010) 024313.

[27] D. He, Z. Peng, W. Gong, Y. Luo, P. Zhao, L. Kong, Mechanism of a green graphene oxide reduction with reusable potassium carbonate, RSC Advances 5 (2015) 11966–11972.

[28] M. I. Araby, M. S. Rosmi, R. Vishwakarma, S. Sharma, Y. Wakamatsu, K. Takahashi, G. Kalita, M. Kitazawa, M. Tanemura, Graphene formation at 150 °C using indium as catalyst, RSC Advances 7 (2017) 47353–47356.

[29] A. Münzer, L. Xiao, Y. H. Sehlleier, C. Schulz, H. Wiggers, All gas-phase synthesis of graphene: Characterization and its utilization for silicon-based lithium-ion batteries, Electrochim. Acta 272 (2018) 52-59.

[30] I. Rodriguez-Pastor, G. Ramos-Fernandez, H. Varela-Rizo, M. Terrones, I. Martin-Gullon, Towards the understanding of the graphene oxide structure: How to control the formation of humic- and fulvic-like oxidized debris, Carbon, 84 (2015) 299–309.

[31] I. Levchenko, M. Keidar, U. Cvelbar, D. Mariotti, A. Mai-Prochnow, J. Fang, K. Ostrikov, Novel biomaterials: Plasma-enabled nanostructures and functions, J. Phys. D: Appl. Phys. 49 (2016) 273001.

[32] S. Guo, S. Dong, Graphene nanosheet: synthesis, molecular engineering, thin film, hybrids, and energy and analytical applications, Chem. Soc. Rev. 40 (2011) 2644–2672.

[33] S. Otles, V. H. Ozyurt. Classical Wet Chemistry Methods. In: Cheung P. (eds) Handbook of Food Chemistry (Springer, Berlin, Heidelberg 2014). https://doi.org/10.1007/978-3-642-41609-5_19-1

[34] G. Kickelbick, A. Betke, Bottom-Up, Wet chemical technique for the continuous synthesis of inorganic nanoparticles, Inorganics 2 (2014) 1-15.

[35] P. J. Rivero, J. A. Garcia, I. Quintana, R. Rodriguez, Design of nanostructured functional coatings by using wet-chemistry methods, Coatings 8 (2017) 76-85.

[36] X. Yao, Y. Song, L. Jiang, Applications of bio-inspired special wettable surfaces, Adv. Mater. 23 (2011) 719–734.

[37] M. Acik, Y. J. Chabal, A review on thermal exfoliation of graphene oxide, J. Mater. Sci. Res. 2 (2013) 101-112.

[38] K. W. Mas'udah, I. M. A. Nugraha, S. Abidin, A. Mufid, F. Astuti, Daminto, Solution of reduced graphene oxide synthesized from coconut shells and its optical properties, AIP Conf. Proc. 1725 (2016) 02004.

[39] H. P. Zhou, X. Ye, W. Huang, M. Q. Wu, L. N. Mao, B. Yu, S. Xu, I. Levchenko, K. Bazaka, Wearable, Flexible, disposable plasma-reduced graphene oxide stress sensors for monitoring activities in austere environments, ACS Appl. Mater. Interfaces 11 (2019) 15122-15132.

[40] I. Levchenko, S. Xu, S. Mazouffre, M. Keidar, K. Bazaka, Mars colonization: Beyond Getting there, Global Challenges 3 (2019) 1800062.

[41] I. Levchenko, M. Keidar, J. Cantrell, Y.-L. Wu, H. Kuninaka, K. Bazaka, S. Xu, Explore space using swarms of tiny satellites, Nature 562 (2018) 185-187.

[42] I. Levchenko, S. Xu, G. Teel, D. Mariotti, M. L. R. Walker, M. Keidar, Recent progress and perspectives of space electric propulsion systems based on smart nanomaterials, Nat. Commun. 9 (2018) 879.

[43] K. Lemmer, Propulsion for CubeSats, Acta Astronaut. 134 (2017) 231-243.

[44] I. Levchenko, K. Bazaka, S. Mazouffre, S. Xu, Prospects and physical mechanisms for photonic space propulsion, Nature Photonics 12 (2018) 649–657.

[45] I. Levchenko, K. Bazaka, Y. Ding, Y. Raitses, S. Mazouffre, T. Henning, P. J. Klar, S.; Shinohara, J. Schein, L. Garrigues *et al.*, Space micropropulsion systems for Cubesats and small satellites: from proximate targets to furthermost frontiers, Appl. Phys. Rev. 5 (2018) 011104.

[46] M. Esmeraldo, A. Gomes, J. Freitas, P. Fechine, S. Sombra, E. Corradini, G. Mele, A. Maffezzoli, S. Mazzetto, Dwarf-green coconut fibers: A versatile natural renewable raw bioresource. Treatment, morphology, and physicochemical properties, Bioresources 5 (2010) 2478-2501.

[47] N. Arena, J. Lee, R. Clift. Life cycle assessment of activated carbon production from coconut shells, J. Cleaner Production 125 (2016) 68-77.

[48] K. Werner, L. Pommer, M. Broström. Thermal decomposition of hemicelluloses, J. Analytic. Appl. Pyrol. 110 (2014) 130-137.

[49] D. Astruc, Why is Ferrocene so Exceptional? Eur. J. Inorg. Chem. 2017 (2017) 6-29.

[50] Š. Toma, R. Šebesta, Applications of ferrocenium salts in organic synthesis, Synthesis 47 (2015) 1683–169.

[51] K. Sa, P. C. Mahakul, B. Das, B. V. R. S. Subramanyam, J. Mukherjee, S. Saha, J. Raiguru, K. C. Patra, K. K. Nanda, P. Mahanandia, Large scale synthesis of reduced graphene oxide using ferrocene and HNO_3, Mater. Lett. 211 (2018) 335–338.

[52] P. Manivel, S. Ramakrishnan, N. K. Kothurkar, N. Ponpandian, D. Mangalaraj, C. Viswanathan, Graphene nanosheets by low-temperature thermal reduction of graphene oxide using RF-CVD, J. Exp Nanosci. 8 (2013) 311–319.

[53] W. Luo, Z. Jian, Z. Xing, W. Wang, C. Bommier, M. M. Lerner, X. Ji, Electrochemically expandable soft carbon as anodes for na-ion batteries, ACS Cent. Sci. 1 (2015) 516−522.

[54] A. Y. Nugraheni, D. N. Jayanti, Kurniasari, S. Soontaranon, E. G. R. Putra, Darminto, Structural analysis on reduced graphene oxide prepared from old coconut shell by synchrotron X-Ray scattering, IOP Conf. Series: Mat. Sci. Eng. 196 (2017) 012007.

[55] C. Fu, G. Zhao, H. Zhang, S. Li, Evaluation and characterization of reduced graphene oxide nanosheets as anode materials for lithium-ion batteries, Int. J. Electrochem. Sci. 8 (2013) 6269 – 6280.

[56] H. Jiang, X. Zhang, W. Gu, X. Feng, L. Zhang, Y. Weng, Synthesis of ZnO particles with multi-layer and biomorphic porous microstructures and ZnO/rGO composites and their applications for photocatalysis, Chem. Phys. Lett. 711 (2018) 100–106.

[57] M. H. Mustafa, A. Zdunek, Supercapacitor nanofiber electrodes graphene-based, Int. J. Electrochem. Sci. 12 (2017) 2917 – 2932.

[58] P. Kumbhakar, A. Pramanik, S. Biswas, A. K. Kole, R. Sarkar, P. Kumbhakar, In-situ synthesis of rGO-ZnO nanocomposite for demonstration of sunlight driven enhanced photocatalytic and self-cleaning of organic dyes and tea stains of cotton fabrics, J. Hazard. Mater. 360 (2018) 193–203.

[59] R. Rajagopal, K. S. Ryu, Synthesis of rGO-doped Nb_4O_5–TiO_2 nanorods for photocatalytic and electrochemical energy storage applications, Appl Catal B. 236 (2018) 125–139.

[60] I. Roy, Synthesis and characterization of graphene from waste dry cell battery for electronic applications, RSC Adv. 6 (2016) 10557.

[61] Y. Jeong, K. Lee, K. Kim, S. Kim, Pore-structure-optimized cnt-carbon nanofibers from starch for rechargeable lithium batteries, Materials 9 (2016) 995.

[62] M. J. Kim, Y. H. Kahng, Y. J. K, T. P. Kumar, K. M. Park, K. Lee, J. H. Jang, Optical endpoint detection for plasma reduction of graphene oxide, AIP Advances 3 (2013) 032121.

Graphene oxide – based supercapacitors from agricultural wastes: a step to mass production of highly efficient electrodes for electrical transportation systems

R. Tamilselvi[1], M. Ramesh[2], G. S. Lekshmi[1], Olha Bazaka[3], Igor Levchenko[4], Kateryna Bazaka[3,4] and M Mandhakini[1*]

[1] *Center for Nanoscience and Technology, Anna University, Chennai, 600 025, India*
[2] *Functional Materials Division, CSIR-Central Electrochemical Research Institute, Karaikudi, 630003, India*
[3] *School of Chemistry, Physics and Mechanical Engineering, Queensland University of Technology, Brisbane, Queensland, 4000, Australia*
[4] *Plasma Sources and Application Centre/Space Propulsion Centre Singapore, NIE, Nanyang Technological University, 637616, Singapore*
[*] *mandhakini7@gmail.com*

Highlights:

Reduced graphene oxide was successfully synthesized from coconut shell and coconut coir

Simple process at low temperature was successfully implemented

Reduced graphene oxide was tested as a super-capacitor electrodes showing very stable performance

This method presents an efficient pathway for synthesis of Reduced graphene oxide for flexible super-capacitor devices